ACCOUNTS
of chemical research

New Aspects of Carrier Multiplication in Semiconductor Nanocrystals

JOHN A. MCGUIRE, JIN JOO, JEFFREY M. PIETRYGA, RICHARD D. SCHALLER, AND VICTOR I. KLIMOV*

Chemistry Division, Los Alamos National Laboratory, Los Alamos, New Mexico 87545

RECEIVED ON MAY 5, 2008

CONSPECTUS

One consequence of strong spatial confinement of electronic wave functions in semiconductor nanocrystals (NCs) is a significant enhancement in carrier−carrier Coulomb interactions. This effect leads to a number of novel physical phenomena including ultrafast decay of multiple electron−hole pairs (multiexcitons) by Auger recombination and high-efficiency generation of mutiexcitons by single photons via carrier multiplication (CM). Significant recent interest in multiexciton phenomena in NCs has been stimulated by studies of NC lasing, as well as potential applications of CM in solar-energy conversion.

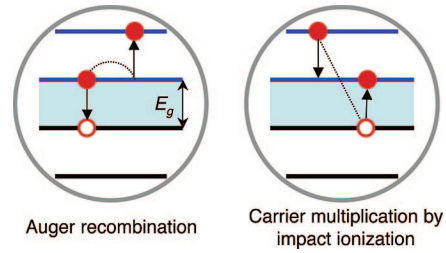

The focus of this Account is on CM. In this process, the kinetic energy of a "hot" electron (or a "hot" hole) does not dissipate as heat but is, instead, transferred via the Coulomb interaction to the valence-band electron, exciting it across the energy gap. Because of restrictions imposed by energy and translational-momentum conservation, as well as rapid energy loss due to phonon emission, CM is inefficient in bulk semiconductors, particularly at energies relevant to solar energy conversion. On the other hand, the CM efficiency can potentially be enhanced in zero-dimensional NCs because of factors such as a wide separation between discrete electronic states, which inhibits phonon emission ("phonon bottleneck"), enhanced Coulomb interactions, and relaxation in translational-momentum conservation.

Here, we investigate CM in PbSe NCs by applying time-resolved photoluminescence and transient absorption. Both techniques show clear signatures of CM with efficiencies that are in good agreement with each other. NCs of the same energy gap show moderate batch-to-batch variations (within ∼30%) in apparent multiexciton yields and larger variations (more than a factor of 3) due to differences in sample conditions (stirred vs static solutions). These results indicate that NC surface properties may affect the CM process. They also point toward potential interference from extraneous effects such as NC photoionization that can distort the results of CM studies.

CM yields measured under conditions when extraneous effects are suppressed via intense sample stirring and the use of extremely low pump levels (0.02−0.03 photons absorbed per NC per pulse) reveal that both the electron−hole creation energy and the CM threshold are reduced compared with those in bulk solids. These results indicate a confinement-induced enhancement in the CM process in NC materials. Further optimization of CM performance should be possible by utilizing more complex (for example, shaped-controlled or heterostructured) NCs that allow for facile manipulation of carrier−carrier interactions, as well as single and multiexciton energies and dynamics.

1. Introduction

Semiconductor nanocrystals (NCs) are nanoscale, crystalline particles that bridge the gap between cluster molecules and bulk materials (Figure 1a).[1] Because of strong spatial confinement of electronic wave functions, electron and hole energies in NCs depend on particle dimensions (the *quantum-size effect*). To a first approximation, this effect can be described by a "quantum box" model,[2,3] which gives rise to a structure of discrete electron and hole energy levels. For a spherical NC with radius R, it predicts a confinement-based contribution to the energy gap proportional to $1/R^2$ (Figure 1b). Through this size-dependent term, the NC energy gap, E_g, can be tuned by more than 1 eV

Published on the Web 11/12/2008 www.pubs.acs.org/acr
10.1021/ar800112v CCC: $40.75

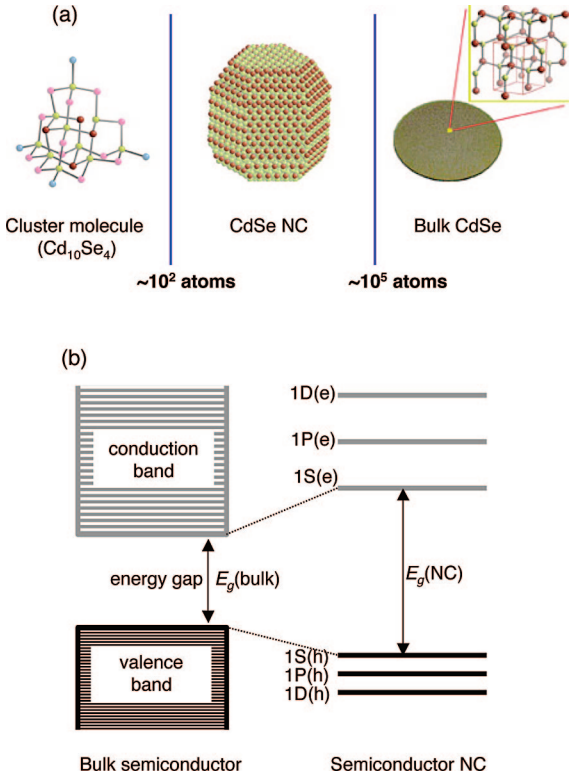

FIGURE 1. (a) NCs (middle) bridge the gap between cluster molecules (left) and bulk materials (right). They contain ~10^2 to ~10^5 atoms per particle. (b) A bulk semiconductor (left) has continuous conduction and valence energy bands separated by a fixed energy gap, E_g, while a semiconductor NC (right) is characterized by discrete atomic-like states and a NC-size-dependent energy gap. Inset: same as the main panel, except linear axes.

for many different compositions, thereby controlling the emission color and the spectral onset of absorption.[4]

An important consequence of strong confinement in NCs is a significant enhancement in carrier−carrier Coulomb interactions resulting from forced overlap of electronic wave functions and reduced dielectric screening associated with interface polarization effects. This enhancement strongly affects carrier dynamics in NCs including intraband relaxation[5−8] and especially multiple electron−hole pair (multiexciton) decay, which becomes dominated by Auger recombination,[9−11] in which the electron−hole recombination energy is released as kinetic energy of a third carrier. Strong carrier−carrier coupling can also result in the generation of multiexcitons by single photons[12,13] known as carrier multiplication (CM). This effect may lead to an appreciable increase in photovoltaic power conversion efficiencies via increased photocurrent.[14−16]

This Account focuses on the photophysics of multiexcitons in semiconductor NCs in the context of CM. The first experimental evidence for high-efficiency CM in quantum-confined

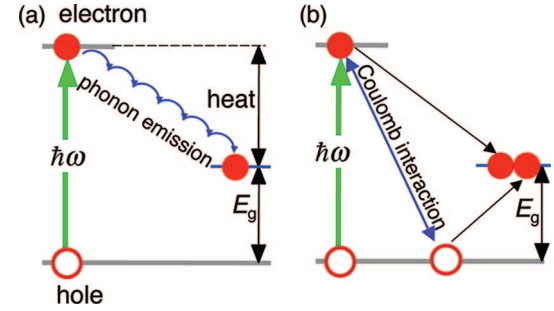

FIGURE 2. (a) Conventional photoexcitation. Absorption of a single photon (green arrow) with energy $\hbar\omega \geq E_g$ produces a single electron−hole pair independent of $\hbar\omega$. In this case, the photon energy in excess of the energy gap is dissipated as heat by exciting phonons (blue arrows). (b) CM via impact ionization. A high-energy conduction-band electron excited by a photon loses its energy by transferring it via the Coulomb interaction to a valence-band electron, which is excited across the energy gap to produce a secondary electron−hole pair.

NCs was provided by spectroscopic studies of PbSe NCs,[12] in which CM was detected on the basis of a distinct decay component due to Auger recombination of multiexcitons.[10] Later, spectroscopic signatures of CM were observed for NCs of other compositions[13,17−20] including an important photovoltaic material Si.[21,22] Further, some indications of CM in photocurrent were observed in PbSe NC device structures.[23−25]

In addition to a large body of experimental data demonstrating high-efficiency CM in NCs, several recent reports have questioned the claim of enhanced CM in NCs, and even its existence, in at least some NC systems.[26−29] The purpose of this Account is to address the apparent controversy regarding CM in NCs and, specifically, to identify some of the reasons for observed discrepancies in the measured CM yields. To establish reliable values of CM efficiencies, here we perform side-by-side studies of CM in solutions of PbSe NCs using two complementary spectroscopic techniques, transient absorption (TA) and time-resolved photoluminescence (PL). To investigate sample-to-sample variations in CM yields, we study NCs prepared by different synthetic routes. We also analyze the impact of processes such as photoinduced formation of surface traps and NC photoionization on apparent CM efficiencies by comparing results for stirred and static solutions.

2. Carrier Multiplication Concept

Conventionally, absorption of a photon with energy $\hbar\omega \geq E_g$ results in a single electron−hole pair (an exciton), while any energy in excess of E_g is dissipated as heat by exciting phonons (Figure 2a). Strong carrier−carrier interactions can, in principle, open a competing carrier generation/relaxation channel in which absorption of a single photon produces two

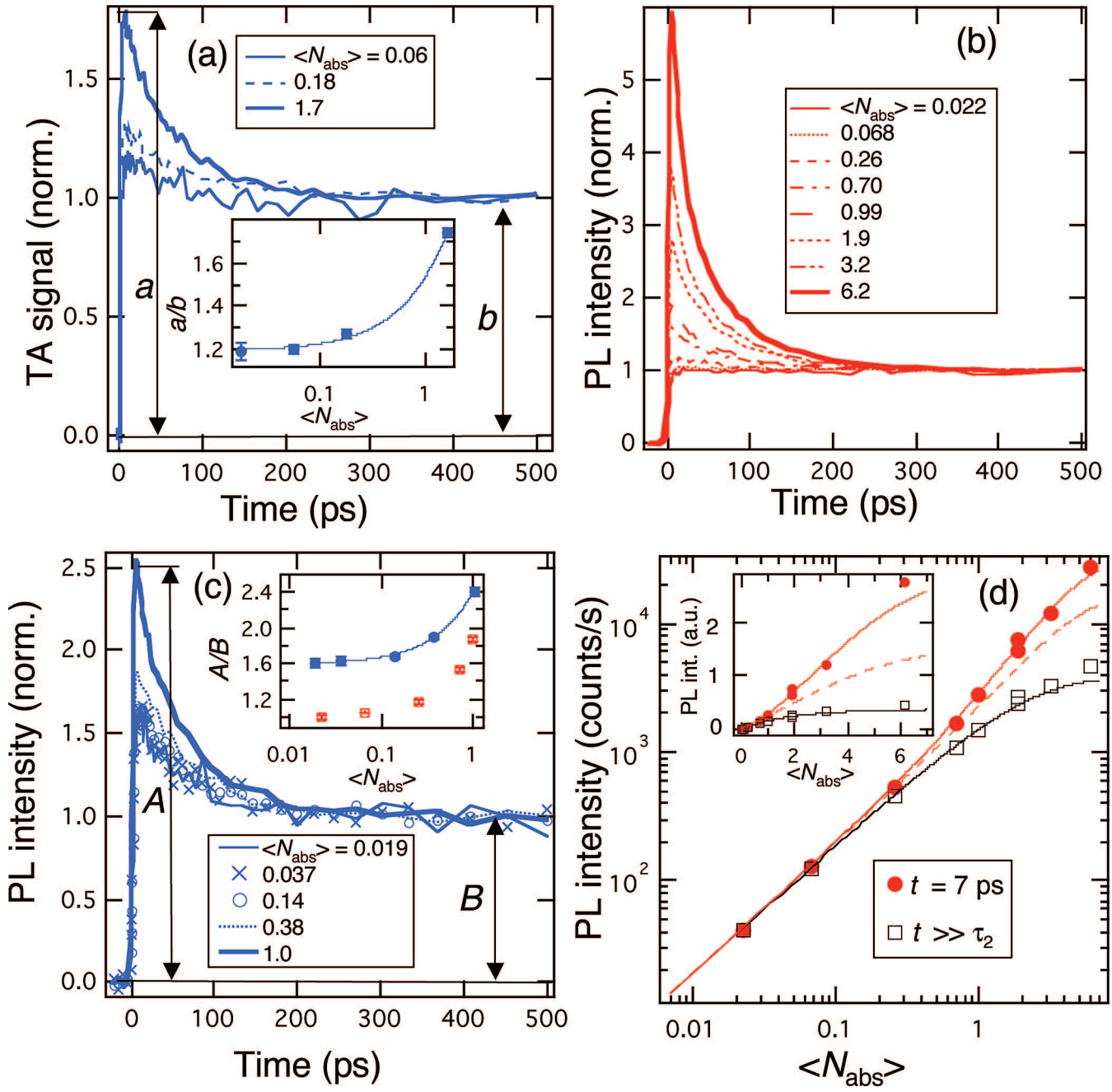

FIGURE 3. Time-resolved spectroscopic studies of PbSe NCs with $E_g = 0.795$ eV (vigorously stirred hexane solution). (a) TA traces normalized at long time after excitation recorded for different pump intensities (indicated in the figure); photon energy is 3.1 eV. Inset: the ratio of the short- to long-time signals (a/b) as a function of $\langle N_{abs} \rangle$ (symbols). The line is a fit assuming the Poisson distribution in the number of absorbed photons; because of CM, the resulting NC occupancies are non-Poissonian. (b) Normalized PL traces as a function of $\langle N_{abs} \rangle$ using excitation at 1.54 eV. (c) Normalized PL traces as a function of $\langle N_{abs} \rangle$ using excitation at 3.08 eV. Inset: The a/b ratio as a function of $\langle N_{abs} \rangle$ for $\hbar\omega = 1.54$ eV (red symbols) and 3.08 eV (blue symbols). The line is a fit to the 3.08 eV data assuming Poissonian photon absorption statistics and the "free-carrier" model of radiative recombination (see text for details). (d) Measured pump-intensity dependences of early- (red circles) and late-time (black squares) PL signals along with theoretical dependences calculated within either the "excitonic" (red dashed line) or the "free-carrier" (red solid line) models assuming that experimentally we can only resolve multiexcitons with $N \leq 3$ (based on measured time constants). The black solid line is a fit of the long-time PL signal to $B \propto r_1(1 - p_0)$.

or more excitons, a process known as CM. In one possible CM scenario (Figure 2b), the excess energy of the conduction band electron does not dissipate as heat but is, instead, transferred to a valence-band electron, exciting it across the energy gap. This process, which can be understood as the reverse of Auger recombination, is known as impact ionization.

In bulk semiconductors, CM is inefficient because of relatively weak Coulomb interactions, the constraints imposed by

translational momentum conservation, and fast phonon emission. The CM efficiency may be enhanced in zero-dimensional NCs because of a wide separation between discrete electronic states, which inhibits phonon emission due to the "phonon bottleneck".[14,30] In addition, stronger Coulomb interactions and relaxation in translational momentum conservation can also contribute to enhanced CM.

Current challenges include understanding of both the mechanism for CM[13,31−37] in NCs and competing energy-loss processes. In bulk materials, CM yields are controlled by the interplay between impact ionization and phonon emission. An additional mechanism competing with CM in NCs is relaxation through interactions with surface ligands, interface defects, or matrix/solvent states. Such *extrinsic* energy relaxation channels may lead to variations in CM efficiencies that depend on NC surface properties.

3. Carrier Multiplication in Transient Absorption and Photoluminescence

Most methods applied to measure CM exploit a significant difference in the recombination dynamics of single excitons and multiexcitons.[12] Single excitons decay via slow radiative recombination (hundreds of nanoseconds in PbSe NCs[38]), while multiexcitons decay on a picosecond time scale via Auger recombination.[10,12,39] Consequently, the generation of multiexcitons by a single photon can be detected via a fast decay component in NC population dynamics.

Earlier studies of CM in PbSe NCs were conducted using primarily TA.[12,13,40] The most recent results obtained using time-resolved PL[29] indicate CM yields that are appreciably lower than those in previous TA studies. To address this discrepancy, here we conduct side-by-side measurements of CM yields in PbSe NCs using TA and PL methods.

In TA studies, we monitor carrier population dynamics by measuring pump-induced bleaching of the lowest-energy 1S absorption feature.[12] In time-resolved PL measurements, we use up-conversion,[41] in which emission from NCs is mixed with a gate pulse (duration from 0.2 to 3 ps) in a nonlinear optical crystal to produce a sum-frequency signal. Unless it is specifically mentioned, below we discuss results obtained for vigorously stirred sample solutions in which the potential effects of processes such as sample photodegradation and NC charging (discussed in the next section) on measured dynamics are reduced.

In TA measurements, CM typically manifests as a fast Auger decay component that persists in the limit of low pump fluences in the case of excitation with photons of high energy ($\hbar\omega > \hbar\omega_{CM}$; $\hbar\omega_{CM}$ is the CM threshold) but vanishes for excitation with low-energy photons ($\hbar\omega < \hbar\omega_{CM}$).[12] An example of such measurements for a sample with $E_g = 0.795$ eV ($\hbar\omega = 3.10$ eV) is shown in Figure 3a. It indicates that a fast mutiexcitonic Auger decay is present even at pump fluences as low as $\langle N_{abs}\rangle \approx 0.02$ (inset of Figure 3a); $\langle N_{abs}\rangle$ is the average number of photons absorbed per NC per pulse at the front face of the sample as estimated from the product of the per-pulse fluence and the NC absorption cross-section (calculated assuming R^3 scaling[42]).

In TA traces, the long-time signal immediately following Auger recombination of multiexcitons (denoted as *b* in Figure 3a) represents a measure of the total number of photoexcited NCs.[12,36] By dividing the early time TA amplitude (*a* in Figure 3a) by *b*, one can determine the average exciton multiplicity, $\langle N_x\rangle$, defined as the average number of excitons per photoexcited NC. The above reasoning is based on the assumption that the 1S bleach scales linearly with the NC occupancy, *N*, which holds until the band-edge states are completely filled ($N = 8$ in PbSe NCs). In the low-intensity limit ($\langle N_{abs}\rangle \rightarrow 0$), $\langle N_x\rangle$ represents a measure of the quantum efficiency (QE) of photon-to-exciton conversion: QE = 100%$\langle N_x\rangle$. From the low-intensity limit of the *a*/*b* ratio in the inset of Figure 3a, we derive QE = 119%, which corresponds to a biexciton yield (η_{xx} = QE − 100) of 19%.

CM is also clearly manifested in PL data. For 1.54 eV excitation, high-intensity PL traces ($\langle N_{abs}\rangle > 1$) show fast initial Auger decay, which vanishes at low pump intensities (Figure 3b). On the other hand, the Auger component persists in the limit of low fluences (down to $\langle N_{abs}\rangle = 0.02$) for excitation with 3.08 eV photons (Figure 3c; mainframe and inset). The latter is consistent with multiexciton generation via CM, which is a single-photon and, hence, pump-intensity-independent process.

4. Multiexciton Radiative Decay Rates: "Excitonic" vs "Free-Carrier" Models

As for TA measurements, the ratio of the early- (*A*) to late-time (*B*) PL signals (Figure 3c) is directly linked to the CM efficiency. However, the relationship between *A*/*B* and QE is more complex than in TA because of a nonlinear scaling of radiative rate constants of *N*-exciton states (r_N) with *N*. To determine this scaling, we analyze the pump-intensity dependence of time-resolved PL signals measured using 1.54 eV excitation (Figure 3d).

To model the PL intensity in PbSe NCs, one must account for the multivalley character of the lead-salt band structure. In

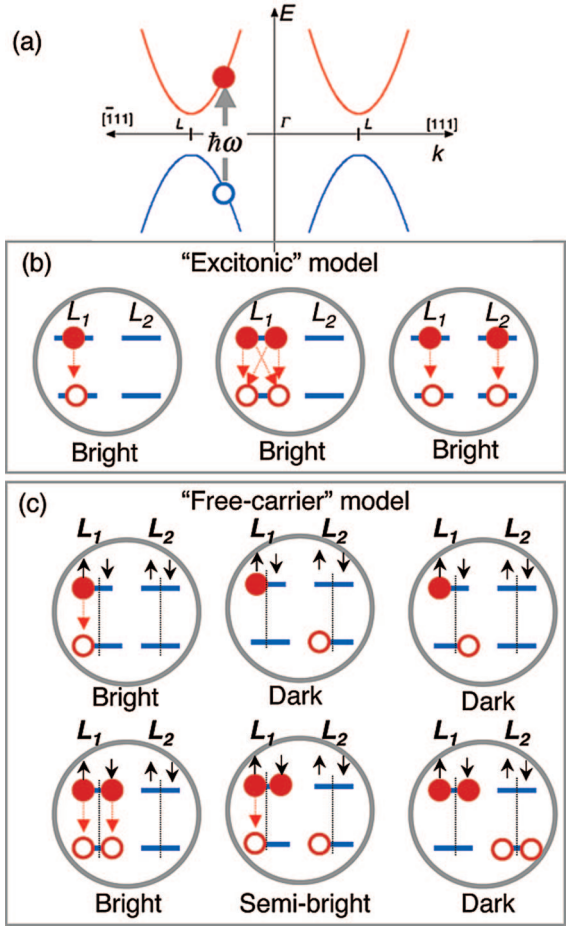

FIGURE 4. (a) Band structure of bulk PbSe; the arrow illustrates an allowed "vertical" interband optical transition. (b) In the "excitonic" model, photoexcitation of a NC produces bright band-edge single excitons (left), as well as bright single-valley (middle) and two-valley (right) biexcitons (red arrows show possible radiative recombination pathways). Here, we assume that because of strong mixing between the conduction- and valence-band states, the electron (hole) spin is not a "good" quantum number and states are, instead, classified according to total angular momentum.[43] (c) In the "free-carrier" model, carriers can occupy with equal probability each of the eight degenerate band-edge states originating from four different band minima with two different spins (black arrows). In this case, one can envision both bright and dark single-exciton states (top row) as well as bright, semibright, and dark biexciton states (bottom row); only a few possible configurations are shown.

PbSe, the conduction- and the valence-band minima are located at four equivalent *L* points of the Brillouin zone (Figure 4a). In NCs, quantum confinement mixes states with different *k*-vectors within the same valley, but intervalley mixing is weak (it becomes important only when the particle size approaches that of a unit cell). Therefore, optical transitions can only occur within the same valley (i.e., "vertically"; arrow in Figure 4a).

Following photoexcitation, carriers can either relax within the same valley (same spin manifold), which would preserve an optically allowed (bright) character in the resulting band-edge excitations ("excitonic" model; Figure 4b) or scatter between states in different valleys or different spins, which in addition to bright species can also produce partially allowed (semibright) and optically passive (dark) species ("free-carrier" model; Figure 4c). In the two latter cases, radiative recombination for at least one electron−hole pair in a NC is forbidden because of either the involvement of intervalley transitions or spin-selection rules. Applying optical selection rules[43] and statistical considerations, we obtain the "excitonic" radiative rate constants scale as 1:14/5:9/2:124/19:17/2:54/5:13:16 for *N* from 1 to 8. Similar considerations predict a N^2 scaling of the "free-carrier" r_N (Figure 3d).

Immediately following Auger recombination, all photoexcited NCs contain single excitons independent of their initial occupancy, and hence, the long-time PL signal can be described by $B \propto r_1(1 - p_0)$, where p_0 is the Poissonian probability of having a nonexcited NC in the ensemble.[42] Using this expression, we fit the pump-intensity dependence of the long-time PL signal (Figure 3d; black line), which yields the effective value of $\langle N_{abs} \rangle$ within the volume probed in PL measurements. We then calculate the Poissonian probabilities of absorbing *i* photons per NC, p_i, and calculate the early time PL intensity from $A \propto \sum_i r_i p_i$ assuming either "excitonic" (red dashed line in Figure 3d) or "free-carrier" (red solid line in Figure 3d) scaling of r_N. The comparison of calculations with the measured data shows that the "free-carrier" model provides a better description of experimental results and indicates that, in PbSe NCs, r_N likely scales as N^2.

5. Carrier Multiplication Yields Derived by Transient Absorption and Photoluminescence: Comparison to Bulk Semiconductors

Assuming quadratic scaling of r_N and considering a system that contains only singly and doubly excited NCs (i.e., single excitons and biexcitons), we obtain the following relationship between $\langle N_x \rangle$ and the *A*/*B* ratio derived from time-resolved PL: $\langle N_x \rangle = (2 + (A/B))/3$. Based on this expression, *A*/*B* of 1.57 measured for the sample in Figure 3c corresponds to $\langle N_x \rangle = 1.19$ (QE = 119%), which is in perfect agreement with the result of TA measurements from Figure 3a.

We have conducted parallel TA and PL studies using ~3.1 eV excitation of samples of several different band gaps, and for all of them, we observe a close correspondence between the CM efficiencies derived by both techniques. These results are plotted in Figure 5 as a function of photon energy ($\hbar\omega$)

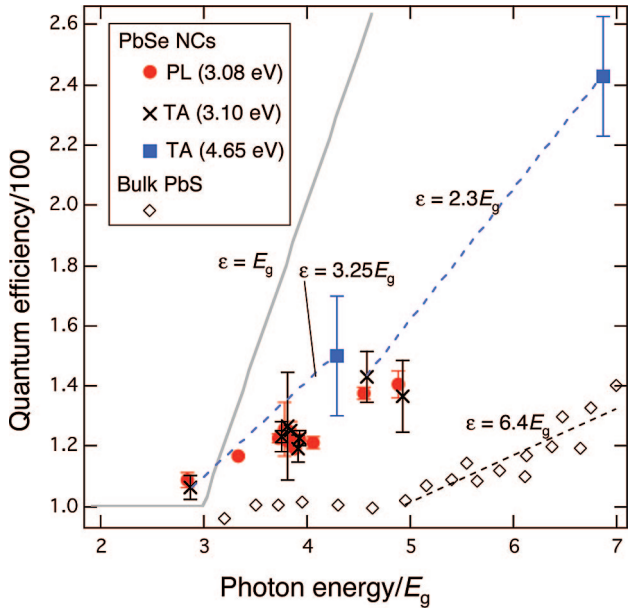

FIGURE 5. Quantum efficiencies of photon-to-exciton conversion derived for PbSe NCs (stirred samples) from time-resolved PL (red circles; $\hbar\omega = 3.08$ eV) and TA (black crosses correspond to $\hbar\omega =$ 3.10 eV and blue squares to 4.65 eV) measurements. Black diamonds are literature data for bulk PbS from ref 44. Gray solid line is the "ideal" QE (see text). The slope of the dashed lines was used to evaluate the electron−hole creation energies, ε, indicated in the figure.

normalized by the energy gap. In this plot, we also include two data points derived from TA measurements conducted with 4.65 eV excitation on stirred solutions of samples with E_g of 1.085 eV (QE = 150%) and 0.63 eV (QE = 245%); the latter QE value implies that CM produces not only biexcitons but also triexcitons.

It is illustrative to compare CM results in NC samples with those in bulk materials. Unfortunately, good quality literature data are unavailable for bulk PbSe, so instead we show in Figure 5 QEs measured for bulk PbS.[44] Since the electronic properties of PbS are similar to those of PbSe, one might expect similar behaviors of these two materials with regard to CM. In addition to the activation threshold, $\hbar\omega_{CM}$, an important characteristic of CM is the electron−hole pair creation energy, ε, which is the energy required to introduce a new exciton into a system.[45] In bulk materials, where QE typically grows linearly with $\hbar\omega$ above $\hbar\omega_{CM}$, ε can be derived from the inverse slope of the QE-vs-$\hbar\omega$ dependence. Based on data from ref 44 in bulk PbS, $\hbar\omega_{CM}$ is ca. $5E_g$, while ε is $\sim 6.4E_g$.

NC-specific effects such as relaxation of momentum conservation and suppressed phonon emission are expected to reduce $\hbar\omega_{CM}$ and ε. Specifically, optical selection rules and the requirement of energy conservation predict that in quantum-confined PbSe NCs the CM threshold can be reduced to $3E_g$,[20] while complete elimination of phonon-related energy losses can potentially decrease ε to the fundamental limit of E_g. These assumptions result in an "ideal" efficiency plot shown in Figure 5 by the gray solid line. One can see that bulk PbS QEs are much lower than "ideal" efficiencies due to large values of $\hbar\omega_{CM}$ and ε. In NCs, both $\hbar\omega_{CM}$ and ε are reduced compared with bulk; as a result, QEs are closer to the "ideal" efficiencies that are defined by energy conservation and optical selection rules. Specifically, the observation of a clearly measurable CM signal down to $2.84E_g$ indicates that the CM threshold in PbSe NCs is below $3E_g$ as was also indicated by previous studies.[12] Further, while the NC data in Figure 5 do not follow a simple bulk-like linear dependence on $\hbar\omega/E_g$, we can still estimate the effective value of ε based on the difference in QEs measured for the same sample for $\hbar\omega = 3.08$ and 4.65 eV. For NCs with $E_g = 0.63$ eV, this estimate yields ε of $2.3E_g$, which is almost 3 times smaller than ε in bulk PbS. These results indicate a confinement-induced enhancement of CM in NCs, as was previously suggested.[12]

6. Variations in Apparent Carrier Multiplication Yields

6.1. Sample-to-Sample Variability. In bulk semiconductors, CM yields are determined by competition between impact ionization and phonon emission. An additional energy-loss mechanism that can compete with CM in NCs is interactions with species at NC interfaces.[46] If surface-related relaxation is important, differences in surface properties may lead to sample-to-sample variations in CM efficiencies even in the case of NCs of the same energy gap.

The effect of sample-to-sample variation is apparent from Figure 6 where we compare PL dynamics for samples with E_g of ~0.8 eV fabricated using two different reducing agents (1,2-hexadecanediol and di-isobutylphosphine) and dispersed in different solvents (hexane and deuterated chloroform). Both samples show nearly "flat" single-exciton dynamics measured using low-intensity 1.54 eV excitation (no CM) (red lines in Figure 6). However, the sample made using di-isobutylphosphine shows a larger fast PL decay component when excited with high-energy photons (3.08 eV; blue lines in Figure 6) indicating a higher CM efficiency (inset of Figure 6). Sample-to-sample variations in multiexciton yields for the NCs used in this study are typically within 30%. One might speculate that greater variations would be observed in the case of a more dramatic difference in NC surface properties, which would, for example, result in distinctly different single-exciton decay dynamics (note that all samples studied here exhibit statistically indistinguishable "flat" single-exciton decay).

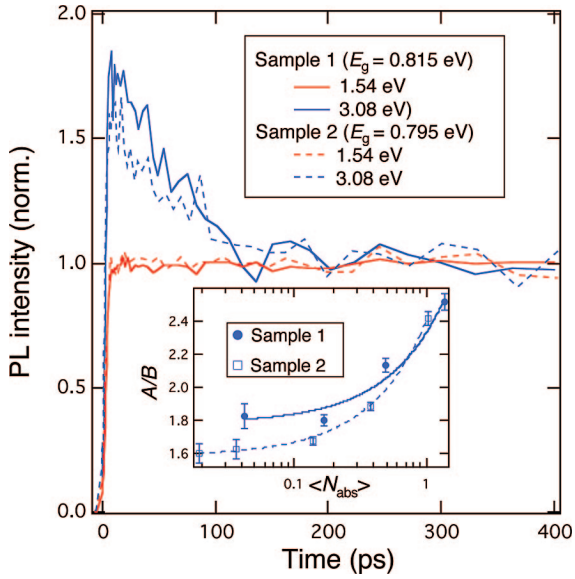

FIGURE 6. Time-resolved PL traces recorded for two stirred PbSe NC samples with a similar energy gap using 1.54 eV (red lines) and 3.08 eV (blue line) excitation. Sample 1 (sample 2) was synthesized using 1,2-hexadecanediol (di-isobutylphosphine) as a reductant and dispersed in deuterated chloroform (hexane). Despite having similar energy gaps, these two samples show an appreciable difference (~30%) in multiexciton yields as indicated by low-intensity limits of the *A*/*B* ratios (inset; $\hbar\omega = 3.08$ eV).

6.2. Stirred vs Static Samples. One practical concern in experimental studies of CM using dynamical techniques is the development of "CM-like" fast decay signatures due to effects such as degradation of surface passivation or NC photoionization leading to NC charging. The former can result in new decay channels due to trapping at surface defects, while the latter can produce extraneous "CM-like" decay components due, for example, to Auger recombination of charged excitons (trions). To evaluate the influence of "CM-like" processes on apparent CM yields, we conduct back-to-back studies of static and stirred NC solutions. In the case of the extremely low fluences used in CM measurements, both of the "extraneous" effects considered above can only develop as a result of exposure to multiple laser pulses. Therefore, they should be suppressed or even eliminated by intense stirring of NC solutions.

While in some cases stirring did not affect the results of TA or PL measurements, some samples showed a significant difference in dynamics measured under static and stirred conditions. A typical effect of stirring is a decrease in the short-time PL amplitude (*A*) accompanied by an increase in the long-time signal (*B*), which results in a decreased *A*/*B* ratio (Figure 7a). The *a*/*b* ratio measured in TA is also reduced upon stirring but in this case primarily because of the increase in the long-time signal (Figure 7b).

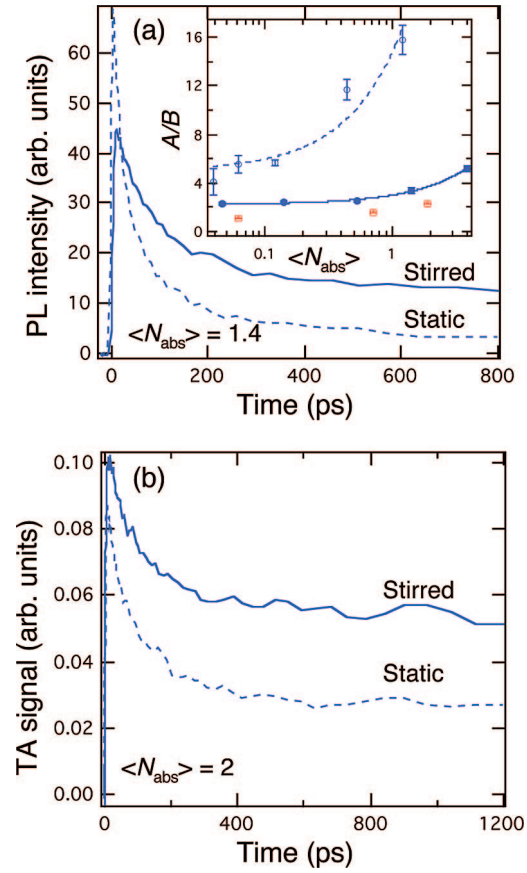

FIGURE 7. (a) PL and (b) TA traces recorded for a stirred (solid lines) and a static (dashed lines) PbSe NC sample with $E_g = 0.63$ eV. Inset in panel a: The low-intensity limit of the *A*/*B* ratio in the static solution is 5.3 versus 2.2 in the stirred solution. An apparent increase in the CM efficiency in the static case is likely not due to an actual increase in the multiexciton yield but rather due to contributions from extraneous processes such as NC ionization (see text for details).

Interestingly, as expected for the CM process, the *A*/*B* and *a*/*b* ratios measured for static solutions show a plateau in the limit of low pump intensities with a magnitude that can greatly exceed that in the stirred case (inset of Figure 7a). This increase, however, is likely *not* indicative of increased CM efficiency. If CM efficiency increased, the long-time "single-excitonic" background would not decrease upon stirring (it is a measure of the total number of photoexcited NCs). The observed difference between the static and stirred measurements cannot be explained by photoinduced formation of surface traps either. The latter effect would reduce the early time PL signal under static conditions, while experimentally we observe the opposite.

A possible explanation of experimental observations invokes photoionization of NCs. Even if this process is of low probability, in the case when uncompensated charges are sufficiently long-lived, it can lead to charging of a large fraction of NCs within the excitation volume of a static solution. In

such a partially charged NC sample, the long-time PL and TA signals are solely due to neutral NCs, and hence, are smaller compared with an all-neutral NC sample. The short-time TA is not expected to significantly change upon NC charging because it represents a measure of the number of excitons injected by the pump pulse (TA is a differential technique). At the same time, the short-time PL signal should increase upon charging because of an increased number of radiative recombination pathways. These trends are indeed observed experimentally indicating that an increase in apparent CM efficiencies under static conditions may result from accumulation of long-lived charges.

6.3. Comparison to Literature Data. The observed sample-to-sample variations in apparent CM yields (particularly large in the case of static samples) may explain a significant spread in published experimental data. For example, a majority of data from initial reports on CM in PbSe NCs[12,13,40] are either above or near the "ideal efficiency" line in Figure 5. In contrast, present measurements of stirred samples indicate efficiencies that are primarily below it. One probable reason for these quantitative discrepancies is the effect of uncontrolled NC charging, which could affect earlier studies since they were conducted on static samples. Further, samples used in earlier works often exhibited fast decay in single-exciton dynamics indicating a significant amount of surface traps. This behavior is different from the nearly "flat" dynamics observed for higher quality samples used in this work, indicating a clear difference in surface properties, which could affect the CM measurements. In earlier works, CM yields could also be overestimated because they were often evaluated from dynamics measured at relatively high fluences ($\langle N_{abs} \rangle$ up to 0.6 in ref 12), for which multiexciton generation via absorption of multiple photons was still significant. Finally, as was pointed out in ref 47, transient spectral shifts of TA features can lead to additional uncertainties in measured CM yields.

A recent TA study conducted on a static sample with E_g = 0.65 eV indicated QEs = 170% for excitation with 3.1 eV photons.[47] This value is comparable to the apparent QEs measured here for static samples with a similar energy gap but higher than that observed for stirred solutions (~140%). This might imply that the results of ref 47 were affected by charging. A recent PL study conducted on stirred PbSe samples with 3.1 eV excitation indicates multiexciton yields from 7% to 23% (QE from 107% to 123%) depending on E_g.[29] These values are lower by ca. a factor of 2 than those measured here by PL under similar conditions. In this case, the observed discrepancies may relate to possible effects of sample surface properties but most likely to differences in experimental details (such as temporal resolution) or the procedures for extracting QEs from the measured PL dynamics. We would like, however, to emphasize that CM yields derived in this work from PL dynamics are consistent with those measured by TA.

7. Summary

CM studies of PbSe NCs indicate clear signatures of multiexciton generation in TA and PL dynamics, and the CM yields derived by these two techniques are in good mutual agreement. For stirred NC solutions, the measured CM efficiencies indicate moderate (~30%) sample-to-sample variations in multiexciton yields for NCs with similar energy gaps, which might reflect the effect of NC surface properties on the CM process. For some samples, we observe a dramatic (more than 3-fold) difference in apparent multiexciton yields measured for NCs under static and stirred conditions. While the exact reasons for this difference still require careful investigations, one potential mechanism involves photoinduced charging of NCs in static solutions. The latter effect can produce extraneous "CM-like" signatures due to Auger recombination of charged single- and multiexciton species and result in overestimations of the measured CM yields.

Measurements conducted under conditions where extraneous effects are suppressed via intense sample stirring and the use of extremely low pump levels (0.02−0.03 photons absorbed per NC per pulse) indicate that both the electron−hole creation energy and the CM threshold in NCs are reduced compared with those in bulk solids. These results confirm the conclusion of previous studies on a confinement-induced enhancement in the CM process in NC materials.

This work was supported by the Chemical Sciences, Biosciences, and Geosciences Division of the Office of Basic Energy Sciences, Office of Science, U.S. Department of Energy (DOE), and Los Alamos LDRD funds. V.I.K. acknowledges partial support by the DOE Center for Integrated Nanotechnologies (CINT) jointly operated by Los Alamos and Sandia National Laboratories. TA measurements were conducted at CINT as part of its user program.

BIOGRAPHICAL INFORMATION

John A. McGuire is a Postdoctoral Research Associate on the "Softmatter Nanotechnology and Advanced Spectroscopy" team in the Chemistry Division of Los Alamos National Laboratory (LANL). He received his Ph.D. (2004) in physics from the University of California, Berkeley. His research interests include the optical properties and ultrafast dynamics of quantum-confined systems.

Jin Joo is a Postdoctoral Research Associate on the "Softmatter" team at LANL. He received his B.S. (1999), M.S. (2001), and Ph.D.

(2005) from Seoul National University, Korea. His current research interests include the synthesis of lead chalcogenide quantum dots and their optical properties.

Jeffrey M. Pietryga is a Technical Staff Member on the "Soft-matter" team at LANL. He received a B.S. in Chemistry from the University of Michigan—Flint (1997), and a Ph.D. in Inorganic Chemistry from the University of Texas (2002). His current research centers on the synthesis and characterization of new infrared-active nanocrystal materials.

Richard D. Schaller is a Technical Staff Member on the "Soft-matter" team at LANL. He received a combined B.A./M.S. (1997) from Northwestern University and his Ph.D. (2002) from University of California, Berkeley. His research interests include nanocrystal photophysics and femtosecond spectroscopies.

Victor I. Klimov is a LANL Fellow and the leader of the "Soft-matter" team in the LANL Chemistry Division. He received his M.S. (1978), Ph.D. (1981), and D.Sc. (1993) degrees from Moscow State University. His current research interests include photophysics of nanocrystal quantum dots, nanoplasmonics, and femtosecond and near-field spectroscopies.

FOOTNOTES

*To whom correspondence should be addressed. E-mail address: klimov@lanl.gov.

REFERENCES

1 Alivisatos, A. P. Semiconductor clusters, nanocrystals, and quantum dots. *Science* **1996**, *271*, 933–937.

2 Efros, A. L.; Efros, A. L. Interband absorption of light in a semiconductor sphere. *Sov. Phys. Semin.* **1982**, *16*, 772–775.

3 Brus, L. E. A simple model for the ionization potential, electron affinity, and aqueous redox potentials of small semiconductor crystallites. *J. Chem. Phys.* **1983**, *79*, 5566–5571.

4 Murray, C. B.; Norris, D. J.; Bawendi, M. G. Synthesis and characterization of nearly monodisperse CdE (E = S, Se, Te) semiconductor nanocrystallites. *J. Am. Chem. Soc.* **1993**, *115*, 8706–8715.

5 Efros, A. L.; Kharchenko, V. A.; Rosen, M. Breaking the phonon bottleneck in nanometer quantum dots: Role of Auger-like processes. *Solid State Commun.* **1995**, *93*, 281–284.

6 Klimov, V. I.; McBranch, D. W. Femtosecond 1P-to-1S electron relaxation in strongly-confined semiconductor nanocrystals. *Phys. Rev. Lett.* **1998**, *80*, 4028–4031.

7 Guyot-Sionnest, P.; Shim, M.; Matranga, C.; Hines, M. Intraband relaxation in CdSe quantum dots. *Phys. Rev. B* **1999**, *60*, 2181–2184.

8 Klimov, V. I.; Mikhailovsky, A. A.; McBranch, D. W.; Leatherdale, C. A.; Bawendi, M. G. Mechanisms for intraband energy relaxation in semiconductor quantum dots: The role of electron-hole interactions. *Phys. Rev. B* **2000**, *61*, 13349–13352.

9 Chepic, D. I.; Efros, A. L.; Ekimov, A. I.; Ivanov, M. G.; Kharchenko, V. A.; Kudriavtsev, I. A.; Yazeva, T. V. Auger ionization of semiconductor quantum drops in a glass matrix. *J. Lumin.* **1990**, *47*, 113–127.

10 Klimov, V. I.; Mikhailovsky, A. A.; McBranch, D. W.; Leatherdale, C. A.; Bawendi, M. G. Quantization of multiparticle Auger rates in semiconductor quantum dots. *Science* **2000**, *287*, 1011–1013.

11 Wang, L.-W.; Califano, M.; Zunger, A.; Franceschetti, A. Pseudopotential theory of Auger processes in CdSe quantum dots. *Phys. Rev. Lett.* **2003**, *91*, 056404.

12 Schaller, R. D.; Klimov, V. I. High efficiency carrier multiplication in PbSe nanocrystals: Implications for solar-energy conversion. *Phys. Rev. Lett.* **2004**, *92*, 186601.

13 Ellingson, R. J.; Beard, M. C.; Johnson, J. C.; Yu, P.; Micic, O. I.; Nozik, A. J.; Shabaev, A.; Efros, A. L. Highly efficient multiple exciton generation in colloidal PbSe and PbS quantum dots. *Nano Lett.* **2005**, *5*, 865–871.

14 Nozik, A. J. Quantum dot solar cells. *Phys. E* **2002**, *14*, 115–120.

15 Hanna, M. C.; Nozik, A. J. Solar conversion efficiency of photovoltaic and photoelectrolysis cells with carrier multiplication absorbers. *J. Appl. Phys.* **2006**, *100*, 074510.

16 Klimov, V. I. Detailed-balance power conversion limits of nanocrystal-quantum-dot solar cells in the presence of carrier multiplication. *Appl. Phys. Lett.* **2006**, *89*, 123118.

17 Murphy, J. E.; Beard, M. C.; Norman, A. G.; Ahrenkiel, S. P.; Johnson, J. C.; Yu, P.; Micic, O. I.; Ellingson, R. J.; Nozik, A. J. PbTe colloidal nanocrystals: Synthesis, characterization, and multiple exciton generation. *J. Am. Chem. Soc.* **2006**, *128*, 3241–3247.

18 Schaller, R. D.; Petruska, M. A.; Klimov, V. I. Effect of electronic structure on carrier multiplication efficiency: Comparative study of PbSe and CdSe nanocrystals. *Appl. Phys. Lett.* **2005**, *87*, 253102.

19 Pijpers, J. J. H.; Hendry, E.; Milder, M. T. W.; Fanciulli, R.; Savolainen, J.; Herek, J. L.; Vanmaekelbergh, D.; Ruhman, S.; Mocatta, D.; Oron, D.; Aharoni, A.; Banin, U.; Bonn, M. Carrier multiplication and its reduction by photodoping in colloidal InAs quantum dots. *J. Phys. Chem. C* **2007**, *111*, 4146–4152.

20 Schaller, R. D.; Pietryga, J. M.; Klimov, V. I. Carrier multiplication in InAs nanocrystal quantum dots with an onset defined by the energy conservation limit. *Nano Lett.* **2007**, *7*, 3469–3476.

21 Beard, M. C.; Knutsen, K. P.; Yu, P.; Luther, J. M.; Song, Q.; Metzger, W. K.; Ellingson, R. J.; Nozik, A. J. Multiple exciton generation in colloidal silicon nanocrystals. *Nano Lett.* **2007**, *7*, 2506–2512.

22 Timmerman, D.; Izeddin, I.; Stallinga, P.; Yassievich, I. N.; Gregorkiewicz, T. Space-separated quantum cutting with silicon nanocrystals for photovoltaic applications. *Nat. Photonics* **2008**, *2*, 105–109.

23 Kim, S. J.; Kim, W. J.; Cartwright, A. N.; Prasad, P. N. Carrier multiplication in a PbSe nanocrystal and P3HT/PCBM tandem cell. *Appl. Phys. Lett.* **2008**, *92*, 191107.

24 Kim, S. J.; Kim, W. J.; Sahoo, Y.; Cartwright, A. N.; Prasad, P. N. Multiple exciton generation and electrical extraction from a PbSe quantum dot photoconductor. *Appl. Phys. Lett.* **2008**, *92*, 031107.

25 Qi, D. F.; Fischbein, M.; Drndic, M.; Selmic, S. Efficient polymer-nanocrystal quantum-dot photodetectors. *Appl. Phys. Lett.* **2005**, *86*, 093103.

26 Nair, G.; Bawendi, M. G. Carrier multiplication yields of CdSe and CdTe nanocrystals by transient photoluminescence spectroscopy. *Phys. Rev. B* **2007**, *76*, 081304.

27 Pijpers, J. J. H.; Hendry, E.; Milder, M. T. W.; Fanciulli, R.; Savolainen, J.; Herek, J. L.; Vanmaekelbergh, D.; Ruhman, S.; Mocatta, D.; Oron, D.; Aharoni, A.; Banin, U.; Bonn, M. Carrier multiplication and its reduction by photodoping in colloidal InAs quantum dots. *J. Phys. Chem. C* **2008**, *112*, 4783–4784.

28 Ben-Lulu, M.; Mocatta, D.; Bonn, M.; Banin, U.; Ruhman, S. On the absence of detectable carrier multiplication in a transient absorption study of InAs/CdSe/ZnSe core/shell1/shell2 quantum dots. *Nano Lett.* **2008**, *8*, 1207–1211.

29 Nair, G.; Geyer, S. M.; Chang, L.-Y.; Bawendi, M. G. Carrier multiplication yields in PbS and PbSe nanocrystals measured by transient photoluminescence. *Phys. Rev. B* **2008**, *78*, 125325.

30 Benisty, H.; Sotomayor-Torres, C. M.; Weisbuch, C. Intrinsic mechanism for the poor luminescence properties of quantum-box systems. *Phys. Rev. B* **1991**, *44*, 10945–10948.

31 Califano, M.; Zunger, A.; Franceschetti, A. Direct carrier multiplication due to inverse Auger scattering in CdSe quantum dots. *Appl. Phys. Lett.* **2004**, *84*, 2409–2411.

32 Califano, M.; Zunger, A.; Franceschetti, A. Efficient inverse Auger recombination at threshold in CdSe nanocrystals. *Nano Lett.* **2004**, *4*, 525–531.

33 Franceschetti, A.; An, J. M.; Zunger, A. Impact ionization can explain carrier multiplication in PbSe quantum dots. *Nano Lett.* **2006**, *6*, 2191–2195.

34 Allan, G.; Delerue, C. Role of impact ionization in multiple exciton generation in PbSe nanocrystals. *Phys. Rev. B* **2006**, *73*, 205423.

35 Shabaev, A.; Efros, A. L.; Nozik, A. J. Multiexciton generation by a single photon in nanocrystals. *Nano Lett.* **2006**, *6*, 2856–2863.

36 Schaller, R. D.; Agranovich, V. M.; Klimov, V. I. High-efficiency carrier multiplication through direct photogeneration of multi-excitons via virtual single-exciton states. *Nat. Phys.* **2005**, *1*, 189–194.

37 Rupasov, V. I.; Klimov, V. I. Carrier multiplication in semiconductor nanocrystals via intraband optical transitions involving virtual biexciton states. *Phys Rev. B* **2007**, *76*, 125321.

38 Wehrenberg, B. L.; Wang, C. J.; Guyot-Sionnest, P. Interband and intraband optical studies of PbSe colloidal quantum dots. *J. Chem. Phys.* **2002**, *106*, 10634–10640.

39 Schaller, R. D.; Petruska, M. A.; Klimov, V. I. Tunable near-infrared optical gain and amplified spontaneous emission using PbSe nanocrystals. *J. Phys. Chem. B* **2003**, *107*, 13765–13768.

40 Schaller, R. D.; Sykora, M.; Pietryga, J. M.; Klimov, V. I. Seven excitons at a cost of one: Redefining the limits for conversion efficiency of photons into charge carriers. *Nano Lett.* **2006**, *6*, 424–429.

41 Shah, J. Ultrafast luminescence spectroscopy using sum frequency generation. *IEEE J. Quantum Electron.* **1988**, *24*, 276–288.

42 Klimov, V. I. Optical nonlinearities and ultrafast carrier dynamics in semiconductor nanocrystals. *J. Phys. Chem. B* **2000**, *104*, 6112–6123.

43 Kang, I.; Wise, F. W. Electronic structure and optical properties of PbS and PbSe quantum dots. *J. Opt. Soc. Am. B* **1997**, *14*, 1632–1646.

44 Smith, A.; Dutton, D. Behavior of lead sulfide photocells in the ultraviolet. *J. Opt. Soc. Am.* **1958**, *48*, 1007–1009.

45 Alig, R. C.; Bloom, S. Electron-hole-pair creation energies in semiconductors. *Phys. Rev. Lett.* **1975**, *35*, 1522–1525.

46 Guyot-Sionnest, P.; Wehrenberg, B.; Yu, D. Intraband relaxation in CdSe nanocrystals and the strong influence of the surface ligands. *J. Chem. Phys.* **2005**, *123*, 074709.

47 Trinh, M. T.; Houtepen, A. J.; Schins, J. M.; Hanrath, T.; Piris, J.; Knulst, W.; Goossens, A. P. L. M.; Siebbeles, L. D. A. In spite of recent doubts carrier multiplication does occur in PbSe nanocrystals. *Nano Lett.* **2008**, *8*, 1713–1718.